CMS Physics Analysis Summary

Contact: cms-pag-conveners-susy@cern.ch 2012/11/29

A Search for Anomalous Production of Events with three or more leptons using 9.2 fb^{-1} of $\sqrt{s}$=8 TeV CMS data

The CMS Collaboration

Abstract

A model-independent search for physics beyond the standard model in events with at least three leptons is presented. The data sample corresponds to 9.2 fb^{-1} of integrated luminosity in pp collisions at $\sqrt{s} = 8$ TeV collected by the CMS experiment at the LHC. Data is binned in exclusive channels. Standard model backgrounds are suppressed by requiring sufficient missing transverse energy, invariant mass inconsistent with that of the Z boson, b-jets, absence of taus, or high jet activity. Control samples in data are used to check the robustness of background evaluation techniques and to minimize the reliance on simulation. The observations are consistent with expectations from standard model processes. These results are used to exclude previously unexplored regions of the supersymmetric parameter space for two representative benchmark scenarios: slepton co-NLSP and a third-generation scenario involving gluino-mediated stop production.

1 Introduction

Supersymmetry (SUSY) is a well known candidate for a theory beyond the standard model (SM) because it solves the hierarchy problem, allows the unification of the gauge couplings, and may provide a candidate particle for dark matter [1–3].

Hadronic collisions yielding three or more electrons, muons, or tau leptons (defining the "multilepton" signature) serve as an ideal hunting ground for physics beyond the SM as such final states are relatively rare in the SM but can be produced frequently in SUSY cascades.

We probe multiple new regions of the supersymmetric parameter space not yet excluded by previous multilepton searches [4–12] using 9.2 fb^{-1} of LHC data collected with the Compact Muon Solenoid (CMS) detector at a centre of mass energy of 8 TeV. The analysis described in this paper is similar in structure to our previous search [13], but uses a dataset with substantially larger integrated luminosity collected at a higher center-of-mass energy. As the search is not tailored to any particular SUSY scenario, its results can be used to constrain a broad range of relevant SUSY models. We demonstrate the sensitivity of this search in the context of two benchmark scenarios that we refer to as "Slepton co-NLSP" and "scenario T1tttt", which are described below.

2 Benchmark Scenarios

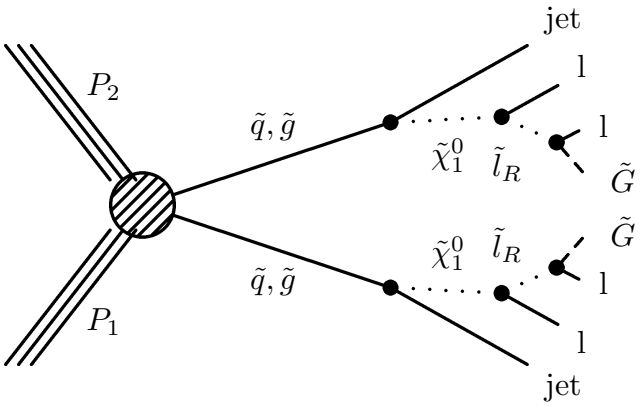

Figure 1: Diagrams of squark or gluino pair production in proton-proton collisions followed by decays leading to a final state with four leptons along with LSPs and jets. Details of the superpartner mass spectrum are described in the text.

Slepton co-NLSP Scenario: Slepton co-NLSP is a model with R-parity conservation, and contains gravitinos as the stable lightest supersymmetric particle (LSP). Scenarios of this type arise in a wide class of theories of gauge mediation with split messengers (GMSM) [14, 15] and can result in multilepton final states [6, 14–16]. The slepton co-NLSP scenario arises in the subset of the GMSM parameter space where the right-handed sleptons are flavor-degenerate.

Figure 1 shows the schematic of the production and decay mechanism for the slepton co-NLSP model. The superpartner mass spectra for these benchmarks are parameterized by the masses for the lightest chargino, $\chi_1^{\pm}$, and the gluino, $\tilde{g}$.The remaining superpartner masses are chosen to be $m_{\tilde{\ell}_R} = 0.3\, m_{\chi_1^{\pm}}$, $m_{\chi_1^0} = 0.5\, m_{\chi_1^{\pm}}$, $m_{\tilde{\ell}_L} = 0.8\, m_{\chi_1^{\pm}}$, and $m_{\tilde{q}} = 0.8\, m_{\tilde{g}}$, with vanishing left-right mixing for the squarks and sleptons, and the Higgsinos decoupled. If $m_{\tilde{g}}$ is moderately low,

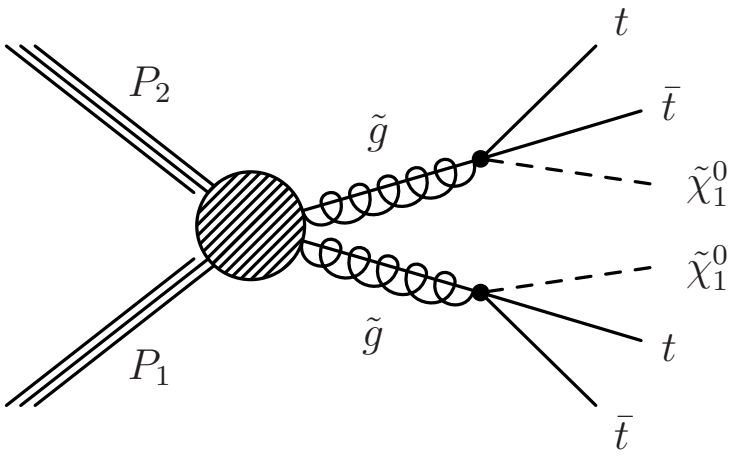

Figure 2: Diagram for decays in the 3rd generation scenario (T1tttt).

strong production dominates and arises through pairs of squarks and gluinos, with cascade decays to the lightest neutralino and jets

$$\widetilde{g} \to \chi_1^0 + \text{jets} \qquad \widetilde{q} \to \chi_1^0 + \text{jets} \tag{1}$$

If instead, the gaugino masses are low, production takes place through chargino-neutralino pairs, with cascade decays to the lightest neutralino

$$\widetilde{\chi}_1^{\pm}, \widetilde{\chi}_2^0 \to \chi_1^0 + W, Z \tag{2}$$

The relative importance of strong and weak production depends on the ratio of gluino to chargino masses. Starting from any production, all cascade decays pass through the lightest neutralino, which decays to the right-handed sleptons

$$\chi_1^0 \to \widetilde{\ell}_R + \ell \tag{3}$$

In the slepton co-NLSP scenario the right-handed sleptons are flavor degenerate, and each decays to the massless Goldstino and a lepton

$$\widetilde{\ell}_R \to \widetilde{G} + \ell \tag{4}$$

Starting from pair production, these cascade decays give events with four leptons, jets, and missing energy. All branching ratios for the cascade decays in the slepton co-NLSP minimal model are supersymmetric.

Third-generation Scenario T1tttt: Scenario T1tttt is a 3rd generation model that involves gluino-mediated stop production and is one of many simplified benchmark models used at the LHC to cover an array of final states. In this scenario, we consider pair-production of gluinos where each gluino undergoes an effective three-body decay in the SMS approximation to $t\tilde{t}$. Each off-shell stop then decays to a $t + \chi_0$ resulting in a final state with four tops [17]. The tops can decay to give multileptonic final states [16, 18].

In addition to frequently containing multiple leptons in the final state, these events also contain four b-tagged jets. The remaining SM background can be significantly reduced by using b-tagging, a new feature of this analysis as compared to its previous version [13].The main

motivation for looking at this model is the solution of the Higgs mass fine-tuning problem if the SUSY particles involved, in particular the gluino and the stop, are light. This motivates the search for stop quarks produced in the decays of gluinos. This is the first search to probe this signature in the multi-lepton final state.

3 Detector and Simulation

The data sample used in this search corresponds to an integrated luminosity of 9.2 fb^{-1} recorded in 2012 with the CMS detector at the LHC. The CMS detector has cylindrical symmetry around the pp beam axis with tracking and muon detector pseudorapidity coverage to $|\eta| < 2.4$, where $\eta = -\ln\tan(\theta/2)$ and θ is the polar angle with respect to the counterclockwise beam. The azimuthal angle ϕ is measured in the plane perpendicular to the beam direction. Charged particle tracks are identified with a 200 m^2, fully silicon-based tracking system composed of a pixel detector with three barrel layers at radii between 4.4 cm and 10.2 cm and a silicon strip tracker with 10 barrel detection layers, of which four are double sided, extending outwards to a radius of 1.1 m. Each system is completed by endcaps extending the acceptance of the tracker up to a pseudorapidity of $|\eta| < 2.5$. The lead-tungstate scintillating crystal electromagnetic calorimeter and brass/scintillator hadron calorimeter hermetically surrounding the tracking system measure the energy of showering particles with $|\eta| < 3.0$. These subdetectors are placed inside a 13 m long and 6 m diameter superconducting solenoid with a central field of 3.8 T. Outside the magnet is the tail-catcher of the hadronic calorimeter followed by the instrumented iron return yoke, which serves as a multilayered muon detection system in the range $|\eta| < 2.4$. The CMS detector has extensive forward calorimetry, extending the pseudorapidity coverage to $|\eta| < 5.0$. The performance of all detector components as measured with cosmic rays has been reported in Ref. [19] and references therein. A much more detailed description of CMS can be found elsewhere [20].

All detector simulations were performed with GEANT4 [21]. The important SM backgrounds for this analysis (Z/γ^* + jets, $t\bar{t}$ quark pairs, and double vector boson production) were generated using MADGRAPH [22]; QCD multijet events were generated with Pythia 8.1 [23]. We use the CTEQ6.6 parton distribution functions [24]. For the dominant WZ+jets contribution up to two jets were selected at the matrix element level in MADGRAPH as the corresponding contributions are not negligible.

The data used for this search came from double-lepton (double-electron, double-muon, muon-electron) triggers. The pt cut-off for these triggers is 17 GeV for the leading lepton and 8 GeV for the next-to-leading lepton. The trigger efficiencies are measured directly using a data sample independently triggered by the sum of hadronic energy in jets (H_T), assuming no correlations between these and the signal triggers.

For electrons and muons with $p_T > 20$ GeV relevant for this analysis, the double-electron, double-muon and muon-electron triggers efficiencies plateau at 99%,92.6%, and 96.9% respectively [25].

We scale each simulated event by the probability for it to satisfy the double-lepton triggers. The uncertainty in the correction to the simulation translates into a systematic uncertainty in the irreducible backgrounds and signal efficiencies.

4 Lepton Identification

This analysis requires the presence of at least three reconstructed lepton candidates. The allowed candidates include electrons, muons and hadronically-decaying taus (τ_h) while leptonic decays of taus (τ_ℓ) are counted as electrons or muons.

We use electrons and muons with $p_{\mathrm{T}} \geq 10$ GeV and $|\eta| < 2.4$. They are reconstructed from measured quantities from the tracker, calorimeter, and muon system. The matching candidate tracks must satisfy quality requirements and spatially match with the energy deposits in the electromagnetic calorimeter and the tracks in the muon detectors, as appropriate. Details of reconstruction and identification can be found in Ref. [26] for electrons and in Ref. [27] for muons. Jets are reconstructed using particles with $|\eta| \leq 2.5$ via the particle-flow (PF) algorithm [28].

The hadronic tau decays yield either a single charged track (one-prong) or three charged tracks (three-prong) with or without additional electromagnetic energy from neutral pion decays as well as neutrinos. In this analysis, we use both one-prong and three-prong hadronic τ decays, reconstructed using the hadron plus strips (HPS) method [29]. We require the visible p_T of the τ to be greater than 20 GeV and $|\eta| \leq 2.3$.

An isolation requirement strongly reduces the background from misidentified leptons, since most of them occur inside jets. We define the relative isolation I_{rel} as the ratio of the sum of the calorimeter energy and p_T of any other tracks in the cone defined by $\Delta R = \sqrt{(\Delta\eta)^2 + (\Delta\phi)^2} < 0.3$ around the lepton to the p_{T} of the lepton. For electrons and muons, we require $I_{\mathrm{rel}} < 0.15$. The sum of energy in the isolation cone is corrected by subtracting out the expected contributions from additional vertices in the event. For the isolation of the hadronic tau decays we require that the sum in a cone of $\Delta R < 0.5$ is less than 2 GeV after excluding the expected contribution from additional overlapping pp interactions in the same or preceding bunch crossing.

Leptons from SUSY decays considered in this search originate from the collision point ("prompt" leptons). After the isolation selection, the most significant background sources are residual non-prompt leptons from heavy quark decays, where the lepton tends to be more isolated because of the high p_{T} with respect to the jet axis. This background is reduced by requiring that the leptons originate from within one centimeter of the primary vertex in z and that the impact parameter d_{xy} between the track and the event vertex in the plane transverse to the beam axis be small: $d_{xy} \leq 0.02$ cm. The isolation and promptness criteria would retain the SUSY signal of prompt leptons, but restrict the background from misidentified leptons to the signal region.

5 Search Strategy

Candidate events in this search must have at least three leptons candidates, where at most one of them is a hadronic τ. The thresholds on the transverse momenta of the leptons are chosen such that triggers used are maximally efficient for selected events. Only electrons and muons are triggered on and the leading muon (electron) is required to have $p_T > 20$ GeV while the next to leading muon (electron) is required to have $p_T > 10$ GeV. The third lepton is required to have $p_T > 10$ GeV for electrons/muons and $p_T > 20$ GeV for taus.

We classify multilepton events into search channels on the basis of the number of leptons, lepton and jet flavor as well as charge and flavor combinations and other kinematic quantities described below. The inclusion of hadronic tau decays in the analysis results in increased background contamination compared to the light leptons case due to higher misidentification rate. To maintain high sensitivity of the analysis, the search channels with tau candidates are kept

separate from pure electron and muon channels.

We classify each event in terms of the maximum number of opposite-sign same flavor (OSSF) dilepton pairs that can be made by using each identified lepton candidate only once. For example, both $\mu^+\mu^-\mu^-$ and $\mu^+\mu^-e^-$ are OSSF1, $\mu^+\mu^+e^-$ is OSSF0, and $\mu^+\mu^-e^+e^-$ is OSSF2. We denote a lepton pair of different flavors as $\ell\ell'$, where ℓ indicates an electron or a muon. The level of SM background varies considerably across the channels. Channels with hadronic tau decays or containing OSSF pairs suffer from larger backgrounds compared to channels with OSSF0. To maximize the overall sensitivity of the search, all these charge combinations are considered as different channels.

We further classify events as containing a leptonically-decaying Z if at least one OSSF pair has reconstructed invariant mass ($m_{\ell^+\ell^-}$) in the Z-mass window, i.e. $|m_{\ell^+\ell^-} - m_Z| < 15$ GeV.

Another criterion for background reduction is the "Z veto", in which the invariant mass of the OSSF lepton pairs is required to be outside the Z-mass window, i.e. $|m_{\ell^+\ell^-} - m_Z| > 15$ GeV. We reject events with $m(\ell^+\ell^-) < 12$ GeV in order to reject low mass Drell Yan and low mass resonances like J/ψ(1S) and Y . In order to remove leptons from conversions (internal and external) that arise from final state radiation from the Z daughters, we reject events where $|m(\ell^+\ell^-) - m_Z| > 15$ GeV but $|m(\ell^+\ell^-\ell'^{\pm}) - m_Z| < 15$ GeV or $|m(\ell^+\ell^-\ell^{\pm}) - m_Z| < 15$ GeV.

An event is considered to contain b-jets if at least one jet passes the b-tagger which uses the CMS "Combined Secondary Vertex algorithm" [30]. The tagger has a tagging efficiency of 70% and a misidentification rate of 13% for the medium working point. We classify events according to the presence or absence of b-jets.

Multilepton signatures benefit from relatively low SM background contamination, which can be further reduced by minimal requirements on either hadronic activity or missing energy above those typical for main SM background contributions. The presence of hadronic activity in an event is characterized by the variable H_T, defined as the scalar sum of the transverse jet energies for all jets with $E_T > 40$ GeV and $|\eta| < 2.5$. Jets used for the H_T determination must be well separated from any identified leptons and this is enforced by requiring no isolated leptons in a cone $\Delta R < 0.3$ around the jet axis. In this search, we classify events as having H_T greater or less than 200 GeV.

The missing transverse energy, E_T^{miss}, is defined as the magnitude of the vectorial sum of the momenta of all particle candidates reconstructed with CMS's Particle Flow [28] algorithm. Comparison between data and simulation shows good modeling of E_T^{miss} for processes with genuine E_T^{miss} from invisible neutrinos [31, 32] as will be shown later. In this search, the E_T^{miss} is divided into 50 GeV wide bins from 0 to 200 GeV and a final bin containing events with $E_T^{miss} \geq 200$ GeV.

In summary, H_T, E_T^{miss} and m_{ll} are good discriminating observables for physics beyond the SM.

6 Background Estimation

6.1 Background from non-prompt leptons

The largest background remaining after the requirement of at least three-lepton candidates originates from the Z+jets process (including Drell-Yan production), in which the Z boson decays leptonically and a third lepton is a result of misidentification from a jet in the event. Since, the QCD component of the simulation cannot be assumed to be reliable as such misidentifica-

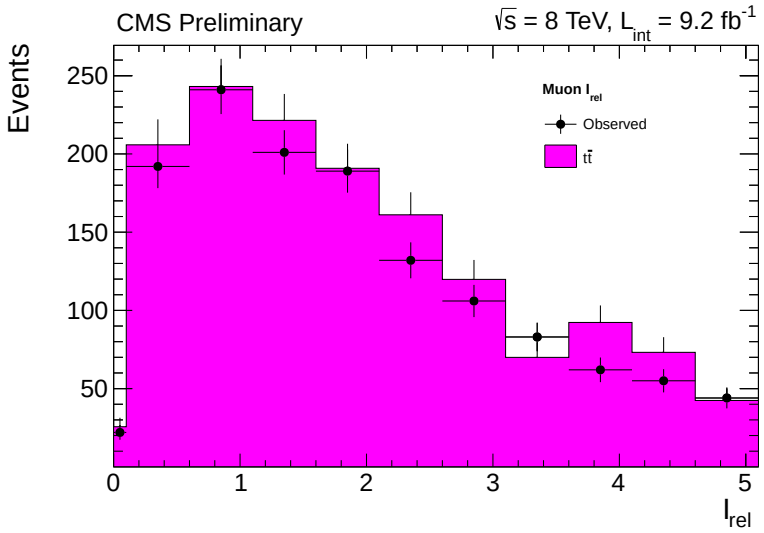

Figure 3: The isolation distribution of muons with large impact parameter ($d_{xy} > 0.02$ cm, primarily from jets) in a data sample enriched in $t\bar{t} \to \ell\nu bbjj$. The last bin contains the overflow.

tions happen when rare fluctuations occur in jet fragmentation, we use data to estimate background contributions from processes with two genuine leptons and one or more misidentified leptons such as $Z(\to 2\ell) + \text{jets}$ and $W^+W^-(\to 2\ell) + \text{jets}$.

To estimate the rate of background contamination from processes with two genuine leptons and a misidentified lepton, we use data with two reconstructed leptons and an additional isolated track scaled by a conversion factor between isolated tracks and lepton candidates from jets. This conversion factor is measured in control samples where no signal is expected to be present, such as in low-$E_{\mathrm{T}}^{\mathrm{miss}}$, low-$H_T$ samples [25]. This method has also been used in the 2011 multilepton analysis [13]. We measure the conversion factor between isolated tracks and muon (electron) candidates to be $0.7\% \pm 0.17\%$ ($0.9\% \pm 0.23\%$) in a data sample dominated by Z+jets and where the systematic uncertainties are one half of the difference between the rates measured in the $\mu^+\mu^-$+isolated track sample and the corresponding rates measured in e^+e^-+isolated track sample. The contribution of the backgrounds with a misidentified third lepton is obtained by multiplying the number of isolated tracks in the sample with two leptons by this conversion factor. In a similar way we estimate the misidentified background for four-lepton events by examining two-lepton events with two isolated tracks. The rates are expected to vary with heavy quark content across the control samples. The variation is accounted for by determining the rate as a function of the impact parameter distribution of non-isolated tracks in the data.

For channels with τ_h, we loosen the isolation requirements to get a conversion factor between loose taus and isolated taus [13, 25]. In particular, we extrapolate the signal region $I < 2\,\text{GeV}$ to a sideband region $6\,\text{GeV} < I < 30\,\text{GeV}$. The ratio of the number of isolated tracks in the two regions is $(15 \pm 3)\%$. We study the variation of this ratio for a number of QCD samples and assign a 30% systematic uncertainty for it. The ratio is applied to the 2ℓ+1 sideband τ event sample.

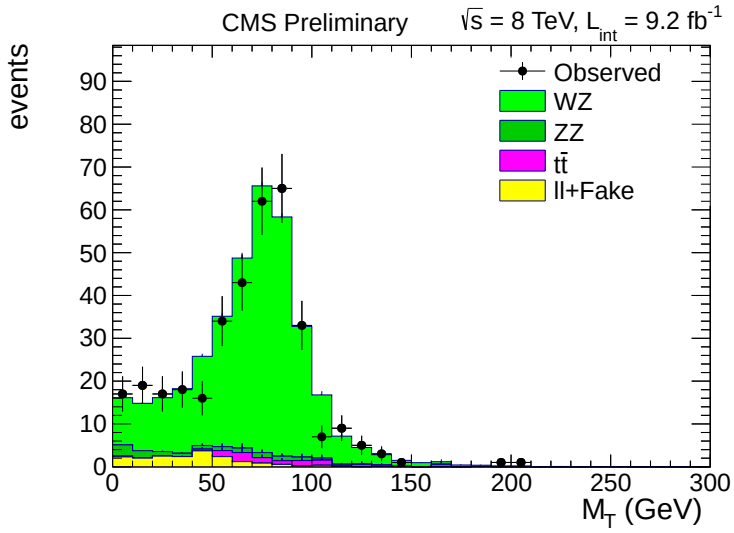

Figure 4: The transverse mass M_T distribution of events in a data sample enriched in WZ requiring an OSSF pair with $m_{\ell\ell}$ in the Z-window and $50\,\text{GeV} < E_{\text{T}}^{\text{miss}} < 100\,\text{GeV}$.

6.2 Background from $t\bar{t}$ Production

This background is estimated from simulation after careful validation in the single lepton and dilepton control regions enriched with $t\bar{t}$. The single lepton control region requires one isolated muon with $p_T > 30$ GeV and at least 3 jets, one of which must satisfy a high efficiency b-tag. Figure 3 shows the distribution of relative isolation of additional non-prompt leptons in the single lepton control region compared to simulation predictions. A good agreement between data and simulation, both in shape and normalization, is observed. The dilepton control region requires an opposite-sign $e-\mu$ pair and is used to compare kinematical variables like S_T, H_T and $E_{\text{T}}^{\text{miss}}$ between data and simulation. In addition, the distribution of the number of jets is reweighted to match data in the dilepton control region.

6.3 Irreducible Background from WZ production

The SM can produce 3 or more genuine prompt leptons with $E_{\text{T}}^{\text{miss}}$ or H_{T} via diboson+jets production where both bosons decay leptonically. This type of background is referred to as "irreducible" because its characteristics are similar to the search signature and is obtained from theory and Monte Carlo simulations.

We correct the simulation to match measured lepton efficiencies [25] and $E_{\text{T}}^{\text{miss}}$ resolution . To correct the $E_{\text{T}}^{\text{miss}}$ resolution, we subdivide the $E_{\text{T}}^{\text{miss}}$ distribution as a function the number of vertices and H_{T} in the event. A large number of vertices in an event indicates a larger extraneous energy in reconstructed objects due to pileup. This stochastic contribution results in larger $E_{\text{T}}^{\text{miss}}$ resolution . On the other hand, a larger H_{T} indicates higher jet activity, leading to systematically larger tails in the $E_{\text{T}}^{\text{miss}}$ distribution due to mis-reconstruction. We model the $E_{\text{T}}^{\text{miss}}$ for events without real $E_{\text{T}}^{\text{miss}}$ (from neutrinos) as a sum of Rayleigh distributions given by

$$p(x) = \sum_{ij} W_{ij} \frac{x}{\sigma_{ij}^2} e^{-x^2/2\sigma_{ij}^2}, \tag{5}$$

where "i" represents the number of vertices in the event and "j" indicates the H_T bin, and the weight W_{ij} is the fraction of events in the bin. Coefficients σ_{ij} are fitted for and characterize the

$E_{\mathrm{T}}^{\mathrm{miss}}$ resolution in both dilepton data and the simulation. We then smear the $E_{\mathrm{T}}^{\mathrm{miss}}$ in simulation on an event by event basis to match the coefficients with data. The magnitude of the correction to the $E_{\mathrm{T}}^{\mathrm{miss}}$ in simulation samples due to the additional smearing varies from a few percent to as high as 25%. The systematic uncertainty is obtained by studying the migration of events due to the additional smearing.

One can then check the simulation against control samples. We verify the simulation by comparing with data samples enriched in WZ-production, the dominant contribution to trilepton signatures from diboson+jets. WZ samples can be selected by requiring three leptons, $50\,\mathrm{GeV} < E_{\mathrm{T}}^{\mathrm{miss}} < 100\,\mathrm{GeV}$, and an on-shell Z i.e. an OSSF pair with the invariant mass satisfying $75\,\mathrm{GeV} < m_{\ell\ell} < 105\,\mathrm{GeV}$ and $H_T < 200$ GeV. Figure 4 shows the tranverse mass between the lepton coming from a W and $E_{\mathrm{T}}^{\mathrm{miss}}$. We scale the WZ Monte-Carlo to match data in the region $50\ \mathrm{GeV} < M_T < 120\ \mathrm{GeV}$ and the scale factor is then used throughout the analysis. In addition, we also reweigh the distribution of the number of jets in the simulation to match the distribution in this control region.

6.4 Backgrounds From Asymmetric Photon Conversions

There are two different types of photon conversions that can give rise to backgrounds in multilepton analyses. The first type is an "external conversion" of an on-shell photon into an $\ell^+\ell^-$ pair in the external magnetic field or material of the detector. This conversion is predominantly into e^+e^- pairs.

The second type of photon conversions are "internal conversions" where the photon is virtual and can produce muons almost as often as electrons. In case of asymmetric conversions, where one lepton has very low p_T and does not pass the selection criteria, Drell-Yan processes with such conversions can lead to a significant background for three lepton signatures.

We choose not to rely on the simulation in evaluating this background contribution because the simulation of such asymmetric internal conversions is unreliable due to the soft lepton p_T being below the generator-level p_T cuts. This motivates data-based measurements of the photon to e/μ conversion factors, measured assuming that the number of on-shell photons undergoing asymmetric conversions is proportional to the number of off-shell photons undergoing asymmetric conversions.

We measure the conversion factors in a control region devoid of new physics (low $E_{\mathrm{T}}^{\mathrm{miss}}$ and low H_{T}). The ratio of the number of events with $|m(\ell^+\ell^-\ell'^{\pm}) - m_Z| < 15$ GeV or $|m(\ell^+\ell^-\ell^{\pm}) - m_Z| < 15$ GeV to the number of events with $|m(\ell^+\ell^-\gamma) - m_Z| < 15$ GeV defines the conversion factor, which is $0.35\% \pm 0.1\%$ ($1.1\% \pm 0.2\%$) for muons (electrons) [13, 25]. The uncertainties are statistical only. We assign systematic uncertainties of 100% to these conversion factors from our underlying assumption of proportionality between virtual and on-shell photons. The measured conversion factors are then used to estimate the background in the signal regions from the observed number of $\ell^+\ell^-\gamma$ events in the signal regions. The background contribution from these converted photons is small after the final selection cuts, as will be shown in the next section.

7 Results and their Interpretation

Tables 1, 2, 3 and 4 show the expected and observed numbers of three- and four-lepton events after the $E_{\mathrm{T}}^{\mathrm{miss}}$ and H_{T} requirements. The different SM background contributions are shown

Selection		MET	N(τ)=0, NbJet=0		N(τ)=1, NbJet=0		N(τ)=0, NbJet$\geq$1		N(τ)=1, NbJet$\geq$1	
			obs	expect	obs	expect	obs	expect	obs	expect
4 Lepton Results $H_T > 200$										
OSSF0	NA	$(100, \infty)$	0	0.007 ± 0.01	0	0.001 ± 0.01	0	0 ± 0.01	0	0 ± 0.009
OSSF0	NA	$(50, 100)$	0	0 ± 0.01	0	0.007 ± 0.01	0	0.01 ± 0.02	0	0.008 ± 0.01
OSSF0	NA	$(0, 50)$	0	1e-05 $\pm$ 0.009	0	0.01 ± 0.01	0	0 ± 0.009	0	0 ± 0.009
OSSF1	off-Z	$(100, \infty)$	0	0.0005 ± 0.009	1	0.09 ± 0.03	0	0.06 ± 0.04	0	0.05 ± 0.03
OSSF1	on-Z	$(100, \infty)$	0	0.03 ± 0.02	0	0.27 ± 0.07	0	0.19 ± 0.11	0	0.17 ± 0.09
OSSF1	off-Z	$(50, 100)$	0	0.03 ± 0.03	1	0.13 ± 0.07	0	0.02 ± 0.02	0	0.07 ± 0.04
OSSF1	on-Z	$(50, 100)$	0	0.08 ± 0.04	1	0.29 ± 0.08	0	0.1 ± 0.06	1	0.12 ± 0.08
OSSF1	off-Z	$(0, 50)$	0	0.007 ± 0.01	0	0.12 ± 0.06	0	0.001 ± 0.01	0	0.04 ± 0.03
OSSF1	on-Z	$(0, 50)$	0	0.1 ± 0.04	0	0.5 ± 0.12	0	0.02 ± 0.02	0	0.23 ± 0.11
OSSF2	off-Z	$(100, \infty)$	0	0.004 ± 0.01	0	0 ± 0	0	0.008 ± 0.01	0	0 ± 0
OSSF2	on-Z	$(100, \infty)$	0	0.05 ± 0.05	0	0 ± 0	0	0.13 ± 0.08	0	0 ± 0
OSSF2	off-Z	$(50, 100)$	0	0.01 ± 0.01	0	0 ± 0	0	0.01 ± 0.02	0	0 ± 0
OSSF2	on-Z	$(50, 100)$	0	0.39 ± 0.1	0	0 ± 0	0	0.16 ± 0.07	0	0 ± 0
OSSF2	off-Z	$(0, 50)$	0	0.11 ± 0.03	0	0 ± 0	0	0.05 ± 0.03	0	0 ± 0
OSSF2	on-Z	$(0, 50)$	2	3.3 ± 0.7	0	0 ± 0	1	0.37 ± 0.09	0	0 ± 0

Table 1: 4-lepton, $H_T > 200$ GeV results from 9.2 fb^{-1} of 2012 data. The labels going down the side refer to whether or not there are OSSF pairs, whether or not $Z \to \ell^+\ell^-$ was excluded (on-Z means m_{ll} between 75 and 105 GeV), and the H_T and MET requirements. Labels along the top of the table give the number of τ candidates, 0 or 1 and the number of b-jets which is 0 or $\geq$1. All channels are exclusive. NOTE: The channels shown in the table are for displaying purposes only. Categorization of events into separate channels used in the fitting procedure uses finer $E_{\mathrm{T}}^{\mathrm{miss}}$ binning. $*$ denotes control channels.

for each channel as well. As a note, categorization of events into separate channels used in the fitting procedure uses finer $E_{\mathrm{T}}^{\mathrm{miss}}$ binning. The channels have been combined into coarse $E_{\mathrm{T}}^{\mathrm{miss}}$ bins to make the table more succinct.

Tables 1, 2, 3 and 4 also show the observations and SM backgrounds in additional control regions, namely the non-signal regions with $E_{\mathrm{T}}^{\mathrm{miss}} < 50$ GeV and/or $H_{\mathrm{T}} < 200$ combined with or without a Z candidate in the event. Furthermore, the channels are classified according to the number of τ candidates as well as the number of b-jets (columns) which shows the larger background for events including hadronic τ decay candidates and no b-jets.

The observed number of events in the channels we examine is largely consistent with expectations. Figure 5 illustrates the comparison of data and expectation for representative channels through $E_{\mathrm{T}}^{\mathrm{miss}}$ distributions in more detail. Since we examine a large number of channels, statistical excursions which would be significant for a single channel search are to be expected.

7.1 Systematic uncertainties and statistical procedures

We discuss the sources of systematic uncertainty and how they impact the search sensitivity before extracting upper limits on the contributions from physics outside the SM. Table 5 lists the salient systematic effects and the resultant uncertainties. All channels share systematic uncertainties for luminosity, renormalization scales, parton distribution functions, and trigger efficiency. The precision in estimating lepton selection efficiencies increases with lepton p_{T}. For a typical slepton co-NLSP signal scenario which has leptons with p_{T} in excess of 20 GeV, the lepton identification and isolation efficiency systematic uncertainty is $\sim$ 1.5% per lepton.

We do a counting experiment with several channels and utilize the broad agreement between the expected SM backgrounds and observations to set limits on the rates of new physics (cross-sections). We use these limits to constrain new physics scenarios and to interpret them in terms of underlying model parameters. The statistical model for the number of events in each channel is a Poisson distribution with expected value, observed value, and log-normal distributions for nuisance parameters. The significant nuisance parameters are the luminosity uncertainty, trigger efficiency, lepton identification efficiencies and background uncertainties. The expected

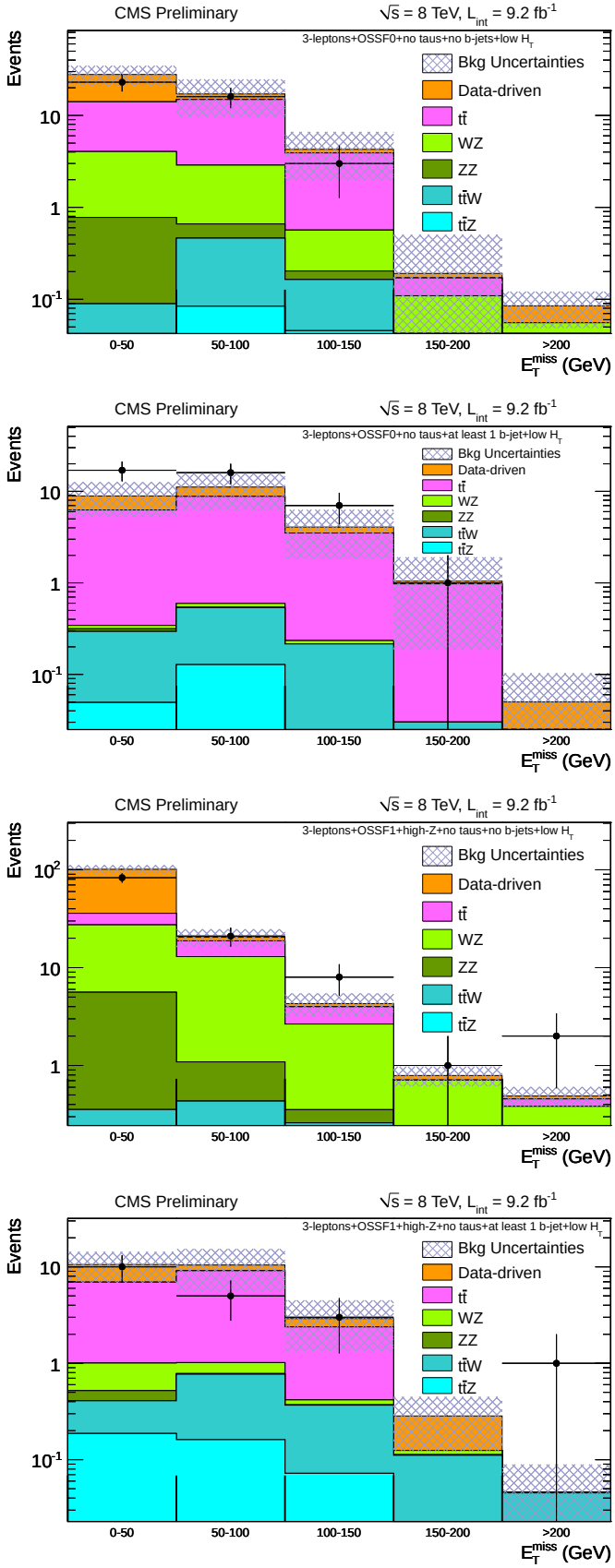

Figure 5: $E_{\mathrm{T}}^{\mathrm{miss}}$ distribution of events with 3-leptons, no OSSF pairs, no taus, $H_T < 200$ GeV and 0 b-jets (first) or $\geq$1 b-jet (second). $E_{\mathrm{T}}^{\mathrm{miss}}$ distribution of events with 3-leptons, one OSSF pair off Z ($>$105 GeV), no taus, $H_T < 200$ GeV and 0 b-jets (third) or $\geq$1 b-jet (fourth). "Data-driven" denotes backgrounds involving two real leptons and a fake lepton. This includes leptons coming from jets, jets faking taus as well as internal asymmetric photon conversions.

Selection		MET	N(τ)=0, NbJet=0		N(τ)=1, NbJet=0		N(τ)=0, NbJet$\geq$1		N(τ)=1, NbJet$\geq$1	
			obs	expect	obs	expect	obs	expect	obs	expect
4 Lepton Results $H_T < 200$										
OSSF0	NA	$(100, \infty)$	0	0.0005 ± 0.009	0	0.5 ± 0.5	0	0 ± 0.009	0	0.04 ± 0.03
OSSF0	NA	$(50, 100)$	0	0.0005 ± 0.009	1	0.17 ± 0.1	0	0 ± 0.009	0	0.11 ± 0.07
OSSF0	NA	$(0, 50)$	0	0.005 ± 0.01	1	0.15 ± 0.07	0	0.001 ± 0.009	0	0.09 ± 0.05
OSSF1	off-Z	$(100, \infty)$	0	0.02 ± 0.01	2	0.18 ± 0.06	0	0.007 ± 0.01	0	0.07 ± 0.04
OSSF1	on-Z	$(100, \infty)$	0	0.18 ± 0.06	1	1 ± 0.18	1	0.15 ± 0.08	0	0.1 ± 0.05
OSSF1	off-Z	$(50, 100)$	0	0.05 ± 0.02	1	0.9 ± 0.3	0	0.02 ± 0.02	0	0.34 ± 0.19
OSSF1	on-Z	$(50, 100)$	1	0.47 ± 0.13	5	3.7 ± 0.6	1	0.15 ± 0.09	0	0.23 ± 0.08
OSSF1	off-Z	$(0, 50)$	1	0.16 ± 0.05	7	3.6 ± 1.1	0	0.04 ± 0.03	0	0.22 ± 0.1
OSSF1	on-Z	$(0, 50)$	1	1.3 ± 0.36	16	18 ± 5.2	0	0.16 ± 0.09	2	0.6 ± 0.22
OSSF2	off-Z	$(100, \infty)$	0	0.01 ± 0.01	0	0 ± 0	0	0.01 ± 0.02	0	0 ± 0
OSSF2	on-Z	$(100, \infty)$	0	0.14 ± 0.07	0	0 ± 0	0	0.26 ± 0.14	0	0 ± 0
OSSF2	off-Z	$(50, 100)$	2	0.05 ± 0.04	0	0 ± 0	0	0.01 ± 0.02	0	0 ± 0
OSSF2	on-Z	$(50, 100)$	1	1.2 ± 0.8	0	0 ± 0	0	0.21 ± 0.09	0	0 ± 0
OSSF2	off-Z	$(0, 50)$	3	3.7 ± 1	0	0 ± 0	1	0.11 ± 0.04	0	0 ± 0
OSSF2	on-Z	$(0, 50)$	76$*$	73 ± 16	0	0 ± 0	3	1.3 ± 0.31	0	0 ± 0

Table 2: 4-lepton, $H_T < 200$ GeV results from 9.2 fb^{-1} of 2012 data. The labels going down the side refer to whether or not there are OSSF pairs, whether or not $Z \to \ell^+\ell^-$ was excluded (on-Z means m_{ll} between 75 and 105 GeV), and the H_T and MET requirements. Labels along the top of the table give the number of τ candidates, 0 or 1 and the number of b-jets which is 0 or $\geq$1. All channels are exclusive. NOTE: The channels shown in the table are for displaying purposes only. Categorization of events into separate channels used in the fitting procedure uses finer $E_{\mathrm{T}}^{\mathrm{miss}}$ binning. $*$ denotes control channels.

Selection		MET	N(τ)=0, NbJet=0		N(τ)=1, NbJet=0		N(τ)=0, NbJet$\geq$1		N(τ)=1, NbJet$\geq$1	
			obs	expect	obs	expect	obs	expect	obs	expect
3 Lepton Results $H_T > 200$										
OSSF0	NA	$(100, \infty)$	1	1.9 ± 1.2	15	7.7 ± 3.6	1	2.9 ± 1.5	27	21 ± 11
OSSF0	NA	$(50, 100)$	1	1.4 ± 0.8	13	17 ± 7.4	1	4.2 ± 1.7	41	37 ± 19
OSSF0	NA	$(0, 50)$	2	1 ± 0.8	13	10 ± 3.4	0	1.9 ± 0.8	32	21 ± 11
OSSF1	above-Z	$(100, \infty)$	2	2.2 ± 0.9	2	4 ± 2.4	3	2.8 ± 1.3	11	6.8 ± 3.7
OSSF1	below-Z	$(100, \infty)$	2	3.5 ± 0.8	8	7.6 ± 3.4	3	3.4 ± 1.6	12	8.3 ± 4.3
OSSF1	on-Z	$(100, \infty)$	17	30 ± 5.3	4	7.9 ± 2.2	5	6.3 ± 1.9	8	5.4 ± 2.8
OSSF1	above-Z	$(50, 100)$	1	1.9 ± 0.49	10	3.7 ± 2.3	4	3.1 ± 1.2	17	12 ± 6.6
OSSF1	below-Z	$(50, 100)$	4	4.5 ± 0.9	11	6.4 ± 2.4	3	5 ± 2.1	9	9.4 ± 5.3
OSSF1	on-Z	$(50, 100)$	39	38 ± 6.2	34	26 ± 5.4	10	9.6 ± 2.7	12	9.5 ± 3.9
OSSF1	above-Z	$(0, 50)$	3	3.2 ± 0.42	19	18 ± 4.5	0	2.7 ± 0.8	6	9.9 ± 4.6
OSSF1	below-Z	$(0, 50)$	9	11 ± 1.2	57	43 ± 10	2	4.7 ± 1.4	11	13 ± 5.3
OSSF1	on-Z	$(0, 50)$	58	63 ± 8.7	256	271 ± 66	12	14 ± 2.6	39	34 ± 7.9

Table 3: 3-lepton, $H_T > 200$ GeV results from 9.2 fb^{-1} of 2012 data. The labels going down the side refer to whether or not there are OSSF pairs, whether or not $Z \to \ell^+\ell^-$ was excluded (below-Z means $m_{ll} < 75$ GeV, above-Z means $m_{ll} > 105$ GeV, on-Z means m_{ll} between 75 and 105 GeV), and the H_T and MET requirements. Labels along the top of the table give the number of τ candidates, 0 or 1 and the number of b-jets which is 0 or $\geq$1. All channels are exclusive. NOTE: The channels shown in the table are for displaying purposes only. Categorization of events into separate channels used in the fitting procedure uses finer $E_{\mathrm{T}}^{\mathrm{miss}}$ binning. $*$ denotes control channels.

value in the model is the sum of the signal and the expected backgrounds.

We set 95% confidence level (C.L.) upper limits on the signal parameters and cross sections using the modified frequentist construction (usually referred to as CLs) [33–35].

The cross-sections for slepton co-NLSP are next-to-leading-order cross sections with the leading-order cross-sections from Pythia and K-factors from Prospino [36]. The cross-sections for the model T1tttt are obtained from [37]. Please see the model discussions in the introduction for more details.

Selection		MET	N(τ)=0, NbJet=0		N(τ)=1, NbJet=0		N(τ)=0, NbJet$\geq$1		N(τ)=1, NbJet$\geq$1	
			obs	expect	obs	expect	obs	expect	obs	expect
3 Lepton Results $H_T < 200$										
OSSF0	NA	$(100, \infty)$	3	4.5 ± 2.3	45	44 ± 22	8	5.1 ± 2.7	41	44 ± 23
OSSF0	NA	$(50, 100)$	16	17 ± 7.5	186	190 ± 63	16	11 ± 4.9	131	119 ± 67
OSSF0	NA	$(0, 50)$	23	27 ± 6.7	429	457 ± 100	17	8.9 ± 3.6	109	115 ± 52
OSSF1	above-Z	$(100, \infty)$	11	5.5 ± 1.2	10	15 ± 8	4	3.1 ± 1.6	10	18 ± 8.2
OSSF1	below-Z	$(100, \infty)$	6	10 ± 3.9	20	23 ± 10	7	7.8 ± 4.1	23	21 ± 11
OSSF1	on-Z	$(100, \infty)$	65	75 ± 11	22	22 ± 5.9	7	5.2 ± 1.9	8	11 ± 5.5
OSSF1	above-Z	$(50, 100)$	21	20 ± 4.2	78	53 ± 17	5	10 ± 4.8	35	39 ± 20
OSSF1	below-Z	$(50, 100)$	66	56 ± 13	167	149 ± 34	26	20 ± 9.7	72	56 ± 27
OSSF1	on-Z	$(50, 100)$	351$*$	368 ± 57	533	457 ± 100	29	18 ± 4.6	40	37 ± 15
OSSF1	above-Z	$(0, 50)$	83	101 ± 9.8	841	845 ± 204	10	10 ± 3.7	65	40 ± 15
OSSF1	below-Z	$(0, 50)$	258	282 ± 29	4820	4113 ± 1018	16	21 ± 6	111	107 ± 27
OSSF1	on-Z	$(0, 50)$	1888$*$	2104 ± 196	24303	22663 ± 5643	65$*$	69 ± 8.8	426	414 ± 99

Table 4: 3-lepton, $H_T < 200$ GeV results from 9.2 fb^{-1} of 2012 data. The labels going down the side refer to whether or not there are OSSF pairs, whether or not $Z \to \ell^+\ell^-$ was excluded (below-Z means $m_{ll} < 75$ GeV, above-Z means $m_{ll} > 105$ GeV, on-Z means m_{ll} between 75 and 105 GeV), and the H_T and MET requirements. Labels along the top of the table give the number of τ candidates, 0 or 1 and the number of b-jets which is 0 or $\geq$1. All channels are exclusive. NOTE: The channels shown in the table are for displaying purposes only. Categorization of events into separate channels used in the fitting procedure uses finer $E_{\mathrm{T}}^{\mathrm{miss}}$ binning. $*$ denotes control channels.

Source of Uncertainty	Uncertainty
Luminosity	4.5%
PDF	14%
Renormalization Scale	10%
$E_{\mathrm{T}}^{\mathrm{miss}}$ Resolution/Smearing: 0-50 GeV, 50-100 GeV, $>$ 100 GeV	(-3%, +4%, +4%)
Jet Energy Scale $W^{\pm}Z$	0.5% (WZ)
B-Tag Veto	0.1% (WZ), 6% ($t\bar{t}$)
Muon ID/Isolation at 10 (100) GeV	11% (0.2%)
Electron ID/Isolation at 10 (100) GeV	14 % (0.6%)
$t\bar{t}$ cross-section/fake rate	50%
WZ cross-section	6%
ZZ cross-section	12%

Table 5: The systematic uncertainties associated with this analysis. The $E_{\mathrm{T}}^{\mathrm{miss}}$ resolution systematic is given for WZ background on Z for different cuts on $E_{\mathrm{T}}^{\mathrm{miss}}$ and for different cuts on M_T given a cut of $E_{\mathrm{T}}^{\mathrm{miss}} > 50$ GeV.

7.2 Exclusion in the Slepton co-NLSP Scenario

In supersymmetry, multilepton final states arise naturally in the subset of GMSM parameter space where the right-handed sleptons are flavor-degenerate and at the bottom of the minimal supersymmetric standard model (MSSM) mass spectrum. The Higgsinos are decoupled. Supersymmetric production proceeds mainly through pairs of squarks and/or gluinos. Cascade decays of these states eventually pass sequentially through the lightest neutralino ($\tilde{g}, \tilde{q} \to \chi^0 + X$), which decays into a slepton and a lepton ($\chi^0 \to \tilde{\ell}^{\pm}\ell^{\mp}$). Each of the essentially degenerate right-handed sleptons promptly decays to the Goldstino component of the almost massless and non-interacting gravitino and a lepton ($\tilde{\ell} \to \tilde{G}\ell$) thus yielding events with four or more hard leptons and missing energy. Such scenarios have a high cross section with little background [16]. The 95% CL exclusion limit for the slepton co-NLSP model is shown in fig. 6. The exclusion curve asymptotes to the horizontal in regions dominated by strong superpart-

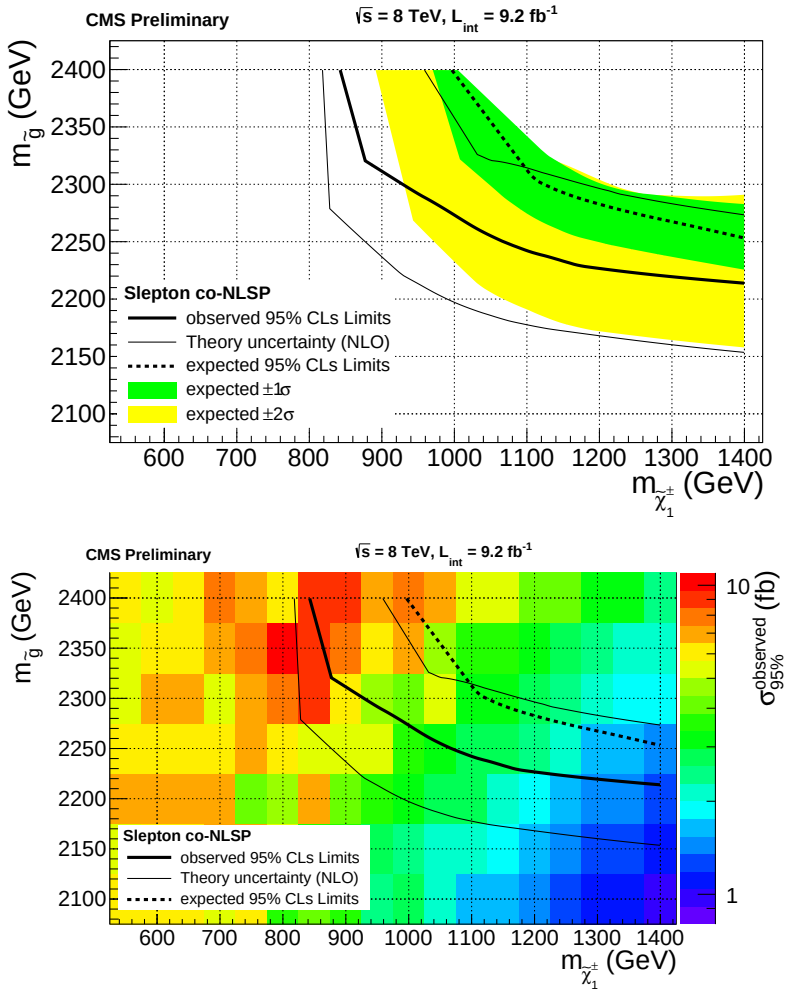

Figure 6: 95% C.L. limits for the slepton co-NLSP scenario as a function of the gluino mass and the wino-like chargino mass are shown. Masses to the left of the curve are excluded. The top figure shows 1σ and 2σ uncertainty bands and the bottom figure shows the observed 95% excluded cross sections in addition.

ner production, and to the vertical in regions dominated by weak superpartner production. With strong superpartners decoupled, the production is dominated by wino-like chargino-neutralino and chargino-chargino production, as well as pair production of sleptons with lower masses that are set by the gauge ordered superpartner mass spectra. The discrepancy between the observed and expected limits at the vertical asymptote is driven by statistical fluctuations in certain channels. More precisely, in the 4-lepton channel with low H_T, OSSF2, off-Z, 0 τ, 0 b-jets and $E_{\mathrm{T}}^{\mathrm{miss}}$ between 50-100 GeV, we see 2 observed events with an expected background of 0.05 events. This statistical fluctuation is the main reason for the discrepancy.

7.3 Exclusion in the 3rd Generation Scenario T1tttt

The simplified model spectra (SMS) have been introduced to produce a given topological signature by limiting the number of particles and decay chains. These models allow comparisons between topologies that are more sensitive to the final state and kinematic selections than the assumptions of a more physically motivated model. One SMS of particular interest is the 3rd

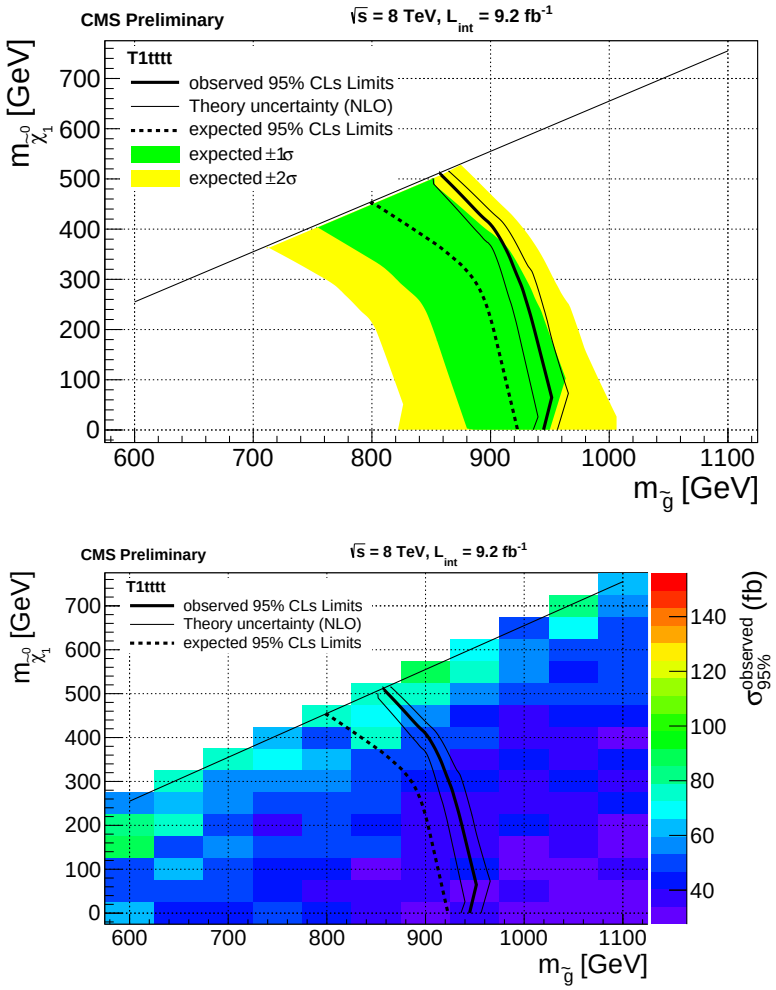

Figure 7: Exclusion limits in the gluino-LSP mass plane for model T1tttt. Masses to the left and below the diagonal line are excluded. The top figure shows 1σ and 2σ uncertainty bands and the bottom figure shows the observed 95% excluded cross sections in addition.

generation model denoted by T1tttt(gluino-mediated stop production), which refers to gluino pair production with the squark decoupled where the gluino directly decays to a ttbar pair and a neutralino (the LSP in this scenario). See figure 2. This scenario is characterized by four top quarks in the final state, which results in four b-jets and four W bosons. Some CMS analyses [38–40] were reinterpreted in this SMS. In addition to producing four b-jets, this model produces large HT and can produce up to four leptons with significant MET. Events with three and four leptons with large HT, large MET, and multiple b-jets have little background. The 95% CL exclusion limits in the gluino-LSP mass plane are shown in fig. 7.

8 Conclusion

We have performed a search for physics beyond the SM using a variety of multilepton final states. We see good agreement between observations and expectations in channels with large SM expectations both on-Z and off-Z.

Taking advantage of the high center-of-mass energy at the LHC, we were able to probe new regions of the slepton co-NLSP and T1tttt models.

References

[1] H. P. Nilles, "Supersymmetry, Supergravity and Particle Physics", *Phys. Rept.* **110** (1984) 1, doi:10.1016/0370-1573(84)90008-5.

[2] H. E. Haber and G. L. Kane, "The Search for Supersymmetry: Probing Physics Beyond the Standard Model", *Phys. Rept.* **117** (1985) 75, doi:10.1016/0370-1573(85)90051-1.

[3] W. de Boer, "Grand unified theories and supersymmetry in particle physics and cosmology", *Prog. Part. Nucl. Phys.* **33** (1994) 201, doi:10.1016/0146-6410(94)90045-0.

[4] CDF Collaboration, "Search for Supersymmetry in $p\bar{p}$ Collisions at $\sqrt{s}$ = 1.96 TeV Using the Trilepton Signature for Chargino-Neutralino Production", *Phys. Rev. Lett.* **101** (2008) 251801, doi:10.1103/PhysRevLett.101.251801.

[5] S. Dube et al., "Addressing the Multi-Channel Inverse Problem at High Energy Colliders: A Model Independent Approach to the Search for New Physics with Trileptons", (2008). arXiv:0808.1605.

[6] J. T. Ruderman and D. Shih, "Slepton co-NLSPs at the Tevatron", (2010). arXiv:1009.1665.

[7] D0 Collaboration, "Search for associated production of charginos and neutralinos in the trilepton final state using 2.3 fb^{-1} of data", *Phys. Lett.* **B680** (2009) 34, doi:10.1016/j.physletb.2009.08.011.

[8] CDF Collaboration, "Search for Supersymmetry in $p\overline{p}$ Collisions at $\sqrt{s} = 1.96$ TeV Using the Trilepton Signature of Chargino-Neutralino Production", (2009). arXiv:0910.1931.

[9] D0 Collaboration, "Search for R-parity violating supersymmetry via the $LL\overline{E}$ couplings λ_{121}, λ_{122} or λ_{133} in $p\bar{p}$ collisions at $\sqrt{s}$ = 1.96 TeV", *Phys. Lett.* **B638** (2006) 441, doi:10.1016/j.physletb.2006.05.077.

[10] CDF Collaboration, "Search for anomalous production of multilepton events in $p\bar{p}$ collisions at $\sqrt{s}$ = 1.96 TeV", *Phys. Rev. Lett.* **98** (2007) 131804, doi:10.1103/PhysRevLett.98.131804.

[11] CMS Collaboration, "Search for Physics Beyond the Standard Model Using Multilepton Signatures in pp Collisions at sqrt(s)=7 TeV", arXiv:1106.0933.

[12] CMS Collaboration, "Search for direct EWK production of SUSY particles in Trilepton final states", *CMS Physics Analysis Summary* **CMS-PAS-SUS-12-006** (2012).

[13] CMS Collaboration, "Search for anomalous production of multilepton events in pp collisions at $\sqrt{s}$=7 TeV", *JHEP* **2012** (2012) doi:10.1007/JHEP06(2012)169.

[14] S. Dimopoulos, S. D. Thomas, and J. D. Wells, "Implications of low energy supersymmetry breaking at the Fermilab Tevatron", *Phys. Rev.* **D54** (1996) 3283, doi:10.1103/PhysRevD.54.3283.

[15] SUSY Working Group Collaboration, "Low-scale and gauge-mediated supersymmetry breaking at the Fermilab Tevatron Run II", (2000). arXiv:hep-ph/0008070.

[16] D. Alves et al., "Simplified Models for LHC New Physics Searches", (2011). arXiv:1105.2838.

[17] CMS Collaboration, "Interpretation of Searches for Supersymmetry", *CMS Physics Analysis Summary* **CMS-PAS-SUS-11-016** (2011).

[18] J. K. e. a. R. Essig, E. Izaguirre, "Heavy Flavor Simplified Models at the LHC", *JHEP* **074** (2012) 1201, doi:10.1007/JHEPD01(2012)074.

[19] CMS Collaboration, "Commissioning of the CMS Experiment and the Cosmic Run at Four Tesla", *JINST* **5** (2010) T03001, doi:10.1088/1748-0221/5/03/T03001.

[20] CMS Collaboration, "The CMS experiment at the CERN LHC", *JINST* **3** (2008) S08004, doi:10.1088/1748-0221/3/08/S08004.

[21] GEANT4 Collaboration, "GEANT4: A simulation toolkit", *Nucl. Instrum. Meth.* **A506** (2003) 250, doi:10.1016/S0168-9002(03)01368-8.

[22] F. Maltoni and T. Stelzer, "MadEvent: Automatic event generation with MadGraph", *JHEP* **02** (2003) 027, doi:10.1088/1126-6708/2003/02/027.

[23] T. Sjöstrand, S. Mrenna, and P. Skands, "A Brief Introduction to PYTHIA 8.1", *Comput. Phys. Commun.* **178** (2008) 852, doi:10.1016/j.cpc.2008.01.036.

[24] P. M. Nadolsky et al., "Implications of CTEQ global analysis for collider observables", *Phys. Rev.* **D78** (2008) 013004, doi:10.1103/PhysRevD.78.013004, arXiv:0802.0007.

[25] CMS Collaboration, "Background and Efficiency Determination Methods for Multilepton Analyses", *CMS Analysis Note* **CMS-AN-2012/257** (2012).

[26] CMS Collaboration, "Electron Reconstruction and Identification at $\sqrt{s} = 7$ TeV", *CMS Physics Analysis Summary* **CMS-PAS-EGM-10-004** (2010).

[27] CMS Collaboration, "Performance of muon identification in pp collisions at $\sqrt{s} = 7$ TeV", *CMS Physics Analysis Summary* **CMS-PAS-MUO-10-002** (2010).

[28] CMS Collaboration, "Commissioning of the Particle-Flow Reconstruction in Minimum-Bias and Jet Events from pp Collisions at 7 TeV", *CMS Physics Analysis Summary* **CMS-PAS-PFT-10-002** (2010).

[29] CMS Collaboration, "Performance of τ-lepton reconstruction and identification in CMS", *Journal of Instrumentation* **7** (2012) doi:no.01,P01001.

[30] CMS Collaboration, "Performance of the b-jet identification in CMS", *CMS Physics Analysis Summary* **CMS-PAS-BTV-11-001** (2011).

[31] CMS Collaboration, "Missing Transverse Energy Performance in Minimum-Bias and Jet Events from Proton-Proton Collisions at $\sqrt{s} = 7$ TeV", *CMS Physics Analysis Summary* **CMS-PAS-JME-10-004** (2010).

[32] CMS Collaboration, "CMS MET Performance in Events Containing Electroweak Bosons from pp Collisions at $\sqrt{s} = 7$ TeV", *CMS Physics Analysis Summary* **CMS-PAS-JME-10-005** (2010).

[33] T. Junk, "Confidence Level Computation for Combining Searches with Small Statistics", *Nucl. Instrum. Meth.* **A434** (1999) 435–443, doi:10.1016/S0168-9002(99)00498-2, arXiv:hep-ex/9902006.

[34] A. L. Read, "Modified frequentist analysis of search results (The CL(s) method)",. Prepared for Workshop on Confidence Limits, Geneva, Switzerland, 17-18 Jan 2000.

[35] A. L. Read, "Presentation of search results: The CL(s) technique", *J. Phys.* **G28** (2002) 2693–2704, doi:10.1088/0954-3899/28/10/313.

[36] W. Beenakker, R. Hoepker, and M. Spira, "PROSPINO: A program for the Production of Supersymmetric Particles in Next-to-leading Order QCD", (1996). arXiv:hep-ph/9611232.

[37] M. Kramer et al., "Supersymmetry production cross sections in pp collisions at $\sqrt{s}$ = 7 TeV", arXiv:1206.2892.

[38] CMS Collaboration, "Search for new physics in events with b-quark jets and missing transverse energy in proton-proton collisions at 7 TeV", *CMS Physics Analysis Summary* **CMS-PAS-SUS-11-006** (2011).

[39] CMS Collaboration, "Search for new physics with same-sign isolated dilepton events with jets and missing energy", *CMS Physics Analysis Summary* **CMS-PAS-SUS-11-010** (2011).

[40] CMS Collaboration, "Search for new physics in events with same-sign dileptons, b-tagged jets and missing energy", *CMS Physics Analysis Summary* **CMS-PAS-SUS-11-020** (2011).